Hindawi
Shock and Vibration
Volume 2022, Article ID 6883663, 10 pages
https://doi.org/10.1155/2022/6883663

Research Article

Dynamic Analysis of a Flexible Multi-Body in 5 MW Wind Turbine

Zhanpu Xue, Hao Zhang, Hongtao Li, Yunguang Ji, and Zhiqiang Zhou

School of Mechanical Engineering, Hebei University of Science and Technology, Shijiazhuang 050018, China

Correspondence should be addressed to Yunguang Ji; jiyg@hebust.edu.cn

Received 4 August 2022; Revised 7 September 2022; Accepted 28 September 2022; Published 17 October 2022

Academic Editor: Tianyou Tao

Copyright © 2022 Zhanpu Xue et al. This is an open access article distributed under the Creative Commons Attribution License, which permits unrestricted use, distribution, and reproduction in any medium, provided the original work is properly cited.

Flexible multi-body dynamics of wind turbines is a subfield of structural mechanics that mainly studies the response of the coupling structure under dynamic loading, such as the transient changes of displacement and stress, in order to measure the load carrying capacity of the coupling structure and obtain the corresponding dynamic properties. Structural dynamics takes into account not only the damping and inertia forces generated by the vibration of the structure but also the elastic force generated by the deformation of the structure. With the continuous increase of individual power and tower height, the flexibility of the multi-body system of wind turbines also increases. The study of the influence of structural parameters on the coupled structural vibrations of tower blades of large wind turbines can provide a scientific basis for the flexible design of large wind turbines as well as important theoretical support for their safe, stable, and economic operation.

1. Introduction

Energy is an important material basis for the survival of human society. In the 21st century, with the continuous development of economic globalization, total energy demand is increasing while traditional energy is gradually decreasing, and the contradiction between supply and demand is becoming more and more obvious. There is an urgent need for the rapid development of renewable energy technologies to solve the increasingly serious energy problem. Wind energy is an environmentally friendly, sustainable, and renewable form of energy. At the same time, it is the fastest growing form of energy in the world. Wind energy is a widely used renewable energy source because of its low cost, mature technology, and high reliability. In recent years, wind energy has developed rapidly in power generation, and power generation has increased year by year and plays an important role.

A two-phase design of the VAWT system is studied. Chen WH conducted the study in two phases, using the Taguchi method to evaluate and optimize the four configurations in the first phase and analyzing specific factors by changing the B value in the second phase [1]. The blade design needs to be optimized to maximize the production efficiency. Hoang Quan Nguyen Ngoc proposes a shape optimization method combining CFD and GA [2]. In studying the seabed response related to the interaction between wave and current, Wei Shuxin used the RANS equation and k-ε turbulence model to simulate fluid dynamics and Biot'sporoelastic theory to simulate the unsteady response of the seabed [3, 4]. Design of a suitable substructure for offshore wind farms, such as conduit racks or multiple piles. Wei Shi performed dynamic time series analysis of each substructure, including deterministic and random load cases [5]. To study the foundation damping and dynamics of OWT monopiles, focusing on the foundation damping analysis, Carswell et al. used the logarithmic decay method of the time interval of free vibration to quantify the critical damping percentage caused by foundation damping in the NREL-5 MW model OWT and compared it with the existing experimental and numerical results [6]. To investigate the wind characteristics and wind energy potential of the three remote islands around Hong Kong, Shu et al. used the Weibull distribution function to estimate the Weibull parameters [7, 8].

In these simulations, Yu-Ting Wu fixed the angular velocity of the rotor blades in advance and compared the calculated thrust coefficient with the turbine manufacturer's information to investigate the possibility of moving the WT after the project was put into operation. To consider the possibility of moving the WT after commissioning, Rodrigues et al. proposed a new framework for layout optimization of moving floating wind farms using an evolutionary optimization strategy in nested configurations [9–10]. To study the improvement of WT performance by two types of roof panels for the rotor blades, Ansari et al. have a three-dimensional program with limited volume to perform periodic numerical simulations of the flow fields of WT at different wind speeds and tilt angles [11, 12]. To analyze the sensitivity of floating offshore wind farms, Laura Castro-Santos considered two different scenarios in her analysis: the life cycle cost of floating offshore wind farms and the main economic indicators in terms of the economic viability of floating offshore wind farms [13]. In selecting the "most appropriate risk mitigation strategy" for offshore wind farms, Mahmood Shafiee used an MSDA method that combines fuzzy set theory and ANP to compare the results of the experimental model [14].

In developing and evaluating the site selection scheme for WTs, Christopher Jung concluded that the most complex scheme should be implemented by considering the site selection strategy of local WTs, analyzing the wind speed wind shear model, and introducing the site selection index for new WTs [15]. In order to estimate the energy performance of a wind farm by analyzing the wind characteristics accurately, a parameter estimation method is used: AMM, Akdağ, and Güler are introduced. Three Weibull distribution parameter estimation methods are used to use the AMM method [16]. To determine the characteristics of the offshore wind energy resource development area by combining wind model data and WT data; analyze the marine meteorological characteristics of the site and select relevant arguments from the existing wind energy floating solutions [17–20]. Ahmad Sedaghat used Weibull distribution to model the wind and power of variable-speed WT. According to the annual average wind speed and form factor, it is found that the WT operation at a low rated wind speed uses a higher rated wind speed [21].

To accurately predict the amount of electricity generated by wind power, Zhao et al. proposed a new multilevel weather forecasting method based on the concept of membership, which introduces a new fuzzy system that can extract the characteristics of these quantities [22]. To solve the problem of joint scheduling of renewable energy and air pollution control in power systems under uncertainty, Chen et al. solved the problem of joint scheduling of renewable energy and air pollution control in power systems under uncertainty, Chen et al. introduced an improved satisfaction-based interactive solution algorithm into the decision process to optimize the constraints of the decision process [23]. To balance the demand-side resources, Zhang et al. proposed a power system scheduling method and established a complete power system load scheduling model to ensure the rational scheduling of renewable energy through the comprehensive optimization of power generation and transmission systems [24]. Zheng et al. build a comprehensive system model of the natural gas and power interconnection system to investigate the important impacts of the wide deployment of renewable energy in the power system on the power system and the tightly coupled system. The results of the case study show that the uncertainty of the power system poses certain operational risks to the operation of the natural gas pipeline system [25]. To account for the intermittent and fuzzy nature of renewable generation, Zhen et al. proposed an imprecise TSFP. The results show that the proposed model can effectively capture the variability of renewable energy and provide an in-depth analysis of the trade-offs between economic goals and systemic risks under various confidence conditions [26–28].

The dynamic response of the flexible multi-body system of a wind turbine is analyzed, and the influence of stress and displacement of structural parameters on the stability of the wind turbine is obtained, which provides a reference value for the state monitoring and control of dynamic parameters during the operation of a wind turbine. The main contents of each part of the paper and the second part is about the research on numerical models of wind turbines and boundary settings. The third part focuses on the application of flexibility theory in wind turbines. In the fourth part, simulation results and analysis are analyzed. The last part is the outlook and summary of this paper.

2. Numerical Model

2.1. Structure Model. As for a 5 MW wind turbine, as an example, the specific values of the structural parameters are as follows: the wind turbine tower is 124 meters high, 2.6 m in diameter, and with a bottom diameter of 4.8 m. The tower is of variable thickness. The structure is divided into three sections; the bottom wall thickness of 150 mm, the top 60 mm wall thickness, and the thickness from bottom to top decreases linearly. The engine room length is 10 m, the width is 4.3 m, the height is 4 m, and the total mass is 136 ∗ 103 kg. The blade is uniformly distributed along the circumferential direction. The rated speed is 17 r/min using finite element analysis software. Use solidworks to build the rigid-flexible coupling three-dimensional structure model, as seen in Figure 1. The tower is a flexible body, the blades are flexible bodies, and the nacelle is a rigid body.

2.2. Numerical Settings. The size of the computational domain is shown in Figure 2. The distance between the inlet and outlet is 10 D. The distance from the inlet boundary to the rotation center of WT is 2.5D. The velocity-pressure split-coupled algorithm is used to solve unsteady RANS, and an implicit two-layer scheme is used for time integration. At the inlet of the computational domain, a uniform atmospheric temperature of 300 K and a velocity of 8.13 m/s are given. At the outlet, the standard atmospheric pressure of 110 kPa is given. The surfaces of the airfoils are nonslip solid walls. Other boundaries are defined as symmetric boundaries. When the aerodynamic load of the wind turbine shows good periodicity, the unsteady calculation can be considered as converged.

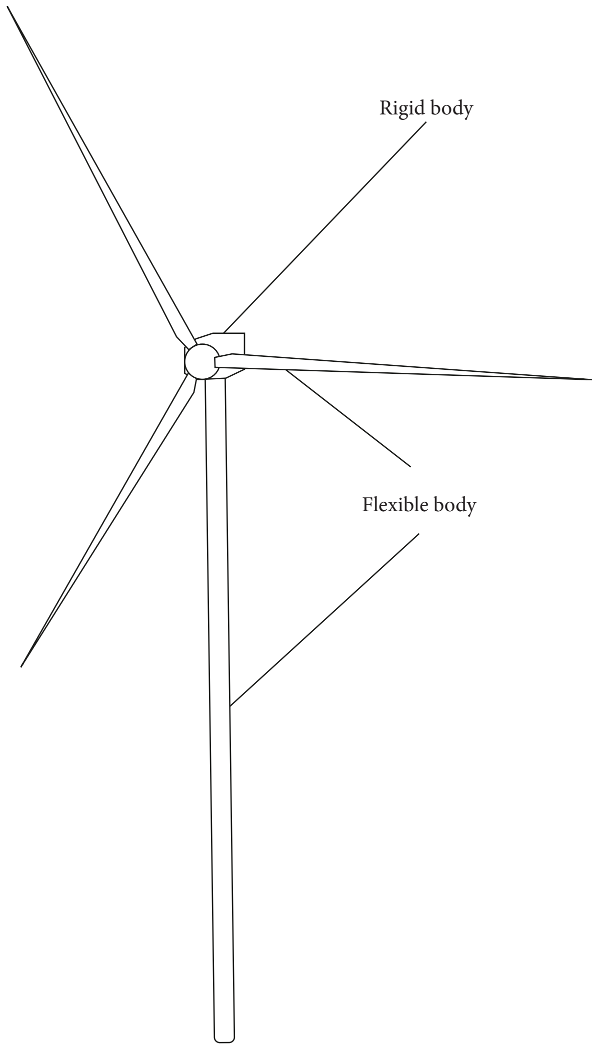

Figure 1: . Three-dimensional model of a rigid-flexible coupling system for a 5 MW wind turbine.

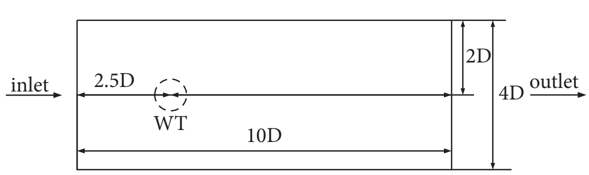

Figure 2: Computational domain of a 5 MW scale wind turbine.

3. Application of Flexibility Theory in Wind Turbines

In the application of flexible theory for coupling structural dynamics analysis of large wind turbines, it is often necessary to make some assumptions and approximations for the dynamic particles of some structures as research objects. On the basis of understanding the dynamic characteristics of flexible multi-body systems, it is necessary to distinguish the main and secondary aspects of structural research. On the premise of ensuring the accuracy of engineering applications, the secondary aspects can be ignored, establishing an efficient coupling structure dynamic model so as to provide research objects with high accuracy in engineering applications. The dynamics of flexible components in the coupling of tower blades with large displacement range movement is studied, and the coupling dynamics mechanism of large displacement range movement and deformation movement is explored.

Because the motion of a large wind turbine coupling structure has the spatial motion characteristics of a flexible multi-body system, and in engineering applications, the mechanical rotation motion of a tower blade coupling structure can be simplified as a structural dynamics problem, which combines the plane motion of a structural point with the spatial motion. The main structural components of large wind turbine coupling have both large rigid motion and deformation motion, and the coupling and interaction of the two motions are the main motion characteristics. As shown in Figure 3, it represents the position vector of point P on the structure of a large wind turbine, where OXY represents the inertial coordinate system and O′ X′ Y′ indicates consolidation at O′ dynamic coordinate system on the micro element of point coupled structure. At this point, the position vector of the P point structure is as follows:

$$r_p = R_{O'} + Au' = R_{O'} + A\left(u_O' + u_f\right) \quad (1)$$

where, u' is the position vector of a certain point of the tower after load deformation in the dynamic coordinate system; $u_o{}'$ is the position vector of a point in the dynamic coordinate system before the tower passes through load deformation; u_f is the elastic deformation vector.

$A = \begin{bmatrix} \cos\theta & -\sin\theta \\ \sin\theta & \cos\theta \end{bmatrix}$ is the rotation transformation matrix of the coupling structure.

The velocity vector p at any point of the flexible body of the tower blade coupling structure is as follows:

$$\dot{r}_p = \dot{R}_{O'} + \dot{A}u' + A\dot{u}', \quad (2)$$

where, A represents the derivative of the rotation matrix with respect to time.

$$\dot{A} = \begin{bmatrix} -\sin\theta & -\cos\theta \\ \cos\theta & -\sin\theta \end{bmatrix}\dot{\theta} = A_\theta\dot{\theta}, A_\theta = \frac{\partial A}{\partial\theta} = \begin{bmatrix} -\sin\theta & -\cos\theta \\ \cos\theta & -\sin\theta \end{bmatrix}. \quad (3)$$

And because $u' = u_f$, then (2) can be expressed in the matrix form as follows:

$$B = \frac{\partial}{\partial\theta}\left(Au'\right) = A_\theta u' \dot{r}_p = \begin{bmatrix} I & B & A \end{bmatrix}\begin{bmatrix} \dot{R}_{O'} \\ \dot{\theta} \\ \dot{u}_f' \end{bmatrix}, \quad (4)$$

where, I means a 2×2 identity matrix.

The P acceleration vector of a particle in a coupled structure can be obtained by deriving from time.

$$\ddot{r}_p = \ddot{R}_{O'} + \ddot{A}u' + 2\dot{A}\dot{u}' + A\ddot{u}', \quad (5)$$

where, $\ddot{A} = \mathrm{d}/\mathrm{d}t\,(A_\theta \dot{\theta}) = \dot{A}_\theta \dot{\theta} + \dot{A}_\theta \ddot{\theta}$ because $A = -\mathrm{A}\theta$, equation (4) can also be expressed as $\ddot{r}_p = \ddot{R}_{O'} + A_\theta u' \ddot{\theta} + A\ddot{u}' + 2\dot{A}\dot{u}' - Au'\dot{\theta}^2$.

The kinetic energy of the tower blade coupling structure is as follows:

$$T = \frac{1}{2}\int_V \rho \dot{r}_P^T \dot{r}_P dV = \frac{1}{2}\dot{q}^T M \dot{q}, \tag{6}$$

where, $q = \begin{bmatrix} \dot{R}_{O'}^T & \dot{\theta}^T & \dot{q}_f^T \end{bmatrix}^T$ is the generalized coordinate of the flexible part of the coupling structure, and M is the mass matrix.

$$M = \int_V \rho \begin{bmatrix} I & B & A\Phi \\ B^T & B^T B & B^T A\Phi \\ \Phi^T A & \Phi^T AB & \Phi^T A^T A\Phi \end{bmatrix} dV. \tag{7}$$

The dynamic equations of the particles in any flexible part of the tower blade coupling structure are assembled with the corresponding matrix, and the corresponding constraint equations are applied. Then the dynamic control equation of the tower blade coupling structure in the flexible multi-body system established by the Lagrange multiplier method is as follows:

$$M^t \ddot{q}^t + K^t q^t + \left(C_q^t\right)^T \lambda = Q_F^t + Q_v^t. \tag{8}$$

The system constraint equation is as follows:

$$C(q, t) = 0 \tag{9}$$

where, the mass matrix M, stiffness matrix K, and Jacobian matrix CQ are respectively

$$M = \begin{bmatrix} M^1 & & & & & \\ & M^2 & & & & \\ & & \ddots & & & \\ & & & M^i & & \\ & & & & \ddots & \\ & & & & & M_{n_b} \end{bmatrix},$$

$$K = \begin{bmatrix} K^1 & & & & & \\ & K^2 & & & & \\ & & \ddots & & & \\ & & & K^i & & \\ & & & & \ddots & \\ & & & & & K_{n_b} \end{bmatrix} \tag{10}$$

$$C_q^T = \begin{bmatrix} C_{q_1}^T \\ C_{q_2}^T \\ \vdots \\ C_{q_i}^T \\ \vdots \\ C_{q_{n_b}}{}^T \end{bmatrix}, Q_F = \begin{bmatrix} Q_F^1 \\ Q_F^2 \\ \vdots \\ Q_F^i \\ \vdots \\ Q_F^{n_b} \end{bmatrix}, Q_v = \begin{bmatrix} Q_v^1 \\ Q_v^2 \\ \vdots \\ Q_v^i \\ \vdots \\ Q_v^{n_b} \end{bmatrix}.$$

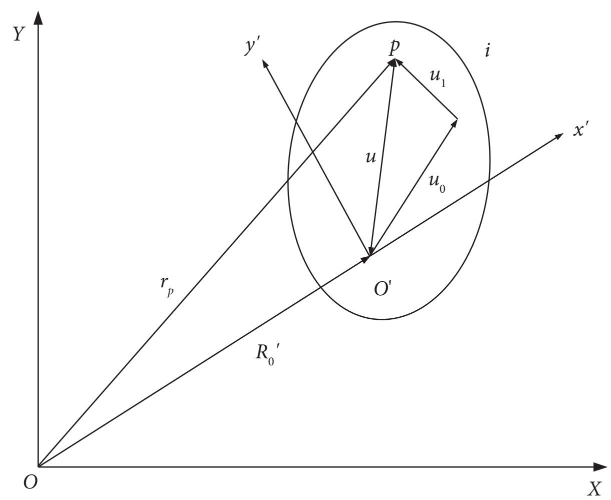

Figure 3: Point structure position vector of a large wind turbine.

The flexible components of large-scale wind turbines are the key components in using wind energy, which are generally composed of a tower, a wind wheel, and other components. However, the transmission system inside the tower plays a certain coupling role in the vibration process, and the requirements for standardization and flexibility of the tower are getting higher and higher in manufacturing. The coupling load is carried by the flexible part of the tower wall, which is affected by air pressure, terrain, and height. The randomness and uncontrollability of the coupling load make the tower's flexibility play a buffer role. The randomness of the coupling load is mainly that the coupling size and direction of the wind load and other loads are constantly changing, and the size of the energy also changes accordingly. Uncontrollable mainly shows that the coupling load cannot be controlled, which directly leads to the diversity of the coupling load, and the response of the flexible parts under the coupling effect is also complicated. In order to accurately analyze the structural dynamics of large-scale wind turbine flexible components, it is necessary to establish a coupling load model in line with the current situation in the process of setting the boundary conditions so as to realize the time history analysis of the coupling load so that the dynamic response can correspond to the change of the load.

The coupled load time history simulation uses the combined wind speed method. Its basic principle is to simplify the wind load into four mathematical models of gust, average wind speed, random wind, and gradual wind through the basic characteristics of the wind load and carry out linear superposition on the basis of satisfying the coupling. The combined wind speed method can use the randomness of the coupling load to establish the corresponding load model, through which the dynamic response time history change of a large-scale wind turbine can be predicted and provide the source coupling load change data for the structural dynamic analysis of the flexible components of a wind turbine. The flexible part of the blade in the wind turbine is affected by its irregular geometric shape, uneven stiffness distribution, uneven section mass distribution, uneven chord length, and thickness distribution along the spanwise direction. The structural dynamics analysis of the flexible part of the blade generally adopts the airfoil section model, which is solved by using the eigenvalues of the dispersion system. The airfoil structure at different positions along the length of the blade is different, so the airfoil model cannot analyze the aeroelastic response of the blade in detail. The aeroelastic analysis can be coupled with aerodynamic damping through the corresponding control equation so that the aeroelastic response can be accurately analyzed. The continuous system model is generally used for the coupling stability of tower blades. By considering the effects of nonlinearity and structural damping, the effects of structural damping, design parameters, bending, and torsion coupling on the aeroelastic stability of blades are discussed, and the aeroelastic problem is transformed into a complex mode problem by using the assumed mode method.

During the normal operation of large-scale wind turbines, the flexible components are subject to coupling loads such as aerodynamic loads, inertia loads, and gravity loads which often form complex load spectra. The coupling effect of towers and blades makes the dynamic response of the wind turbine during its rotation period a curve that changes with time. The situation at the wind farm is complex and changeable. Under the action of coupling loads, the structural organization of mechanical materials may change, causing structural failure and resulting in the normal operation of flexible components. Therefore, it is necessary to monitor the dynamic response of flexible components under coupling loads. Under normal wind speeds, large-scale wind turbines can obtain the maximum power coefficient and improve the wind energy capture ability by adjusting the blade tip speed ratio. However, as the main component, the flexible component of the wind turbine needs to track and control the wind energy. The continuous improvement of energy demand drives the development of the wind power industry, and the efficient use of wind resources has become one of the hot issues. The structural dynamic analysis of flexible components of large-scale wind turbines is the premise of efficient use of wind resources.

With the increasing volume and weight of large-scale wind turbines, higher requirements are put forward for the control system, and the flexible components are gradually developing towards intelligence. The application of flexibility theory plays a basic role in monitoring and controlling the dynamic parameters of the large-scale wind turbine tower blade coupling structure. Flexible components can adapt to the coupling of structure and load, and the structural dynamic parameters show a good change trend. Flexible towers and blades are the inevitable trend of large-scale wind turbine manufacturing.

The application of tower blade coupling structural dynamics is mainly aimed at the stress and displacement analysis when the structure bears dynamic load. Its essence is the extension of the structural analysis method for static load, which regards static load as a special form of dynamic load. However, in the linear and nonlinear structural analysis, in order to calculate more accurately, the two loads are calculated separately, and then the numerical simulation results are superimposed to obtain an accurate solution. A dynamic load is a load whose magnitude and direction change with time. The structural response of dynamics is mainly expressed as displacement and stress, while the structural response of structural dynamics is mainly measured by the displacement of the structure. Other responses of the structure, such as impact and internal force, are secondary aspects of the analysis.

4. Simulation Results and Analysis

Take a point at the blade tip and root, respectively and observe the stress value and displacement value of the two points under different wind speeds, as shown in Figures 4 and 5. When the wind speed is less than 3.5 m/s, the stress value of the blade root increases with the increase in wind speed and reaches its maximum value of 6.258×10^2 Pa at 3.5 m/s. When the wind speed is greater than 3.5 m/s, the stress value of the blade root drops sharply and increases slowly with the increase in wind speed. The tip stress value has no obvious change when the wind speed is 2 m/s, 2.5 m/s, and 3 m/s. When the wind speed is greater than 3.5 m/s, the tip stress value drops to near 0. The maximum stress curve at each wind speed is shown in Figure 5. The maximum stress increases gradually with the increase in wind speed. When the wind speed is 13.8 m/s, the maximum stress is 2.527×10^6 Pa.

The displacement curves of the blade tip and root under different wind speeds are shown in Figure 6. The displacement values of blade tip and root increase with the increase in wind speed, and the displacement value of blade tip is always greater than that of blade root. When the wind speed is 6 m/s, the displacement value decreases, which is the local lowest point. When the wind speed is greater than 6 m/s, the displacement value gradually increases and reaches its maximum value when the wind speed is 13.8 m/s. The maximum displacement curve under different wind speeds is shown in Figure 7. When the wind speed is 3 m/s, there is a local maximum of 33.15 mm.

From Figures 8–11, we show the breeze state. The maximum stress value of the wind turbine is 2744 Pa in Figure 8, which is located at the blade tip. The stress value at the middle and trailing edge of the blade is relatively small, and the stress range is 1098 Pa–2195 Pa. The stress value at other positions of the wind turbine is small, and the maximum displacement value is 3.451 mm, which is the same as the maximum stress position, and the displacement gradually decreases with the decrease in the distance from the hub. In Figure 9, the maximum stress value of the wind turbine is 3485 Pa, which is located at the blade tip. The stress value at the middle and trailing edge of the blade is relatively small, and the stress range is 2532 Pa–5063 Pa. The stress value at other positions of the wind turbine is small, and the maximum displacement value is 7.959 mm, which is the same as the maximum stress position. The displacement decreases gradually with the decrease of the distance from the hub, and the displacement between the hub and the engine room area is 1.990 mm.

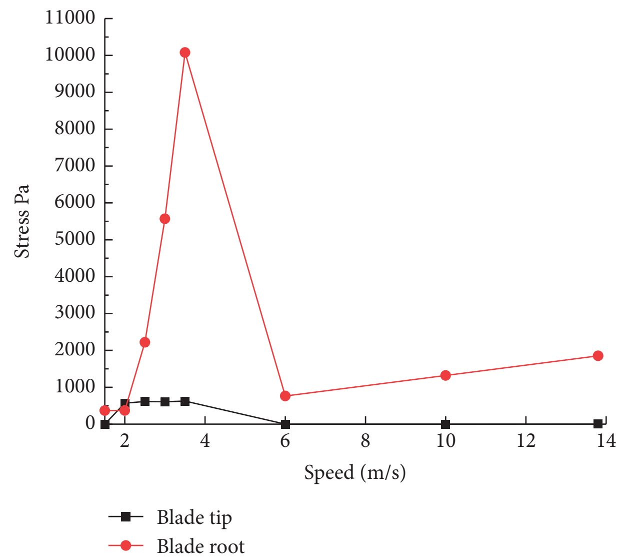

Figure 4: Stress value curve of the blade tip and blade root.

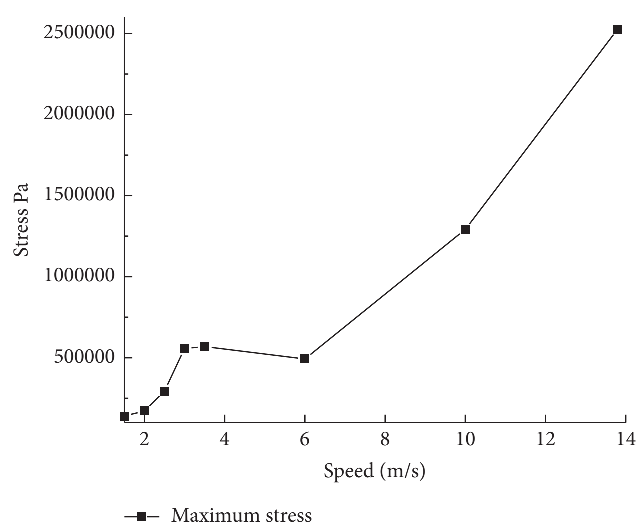

Figure 5: Maximum stress curve.

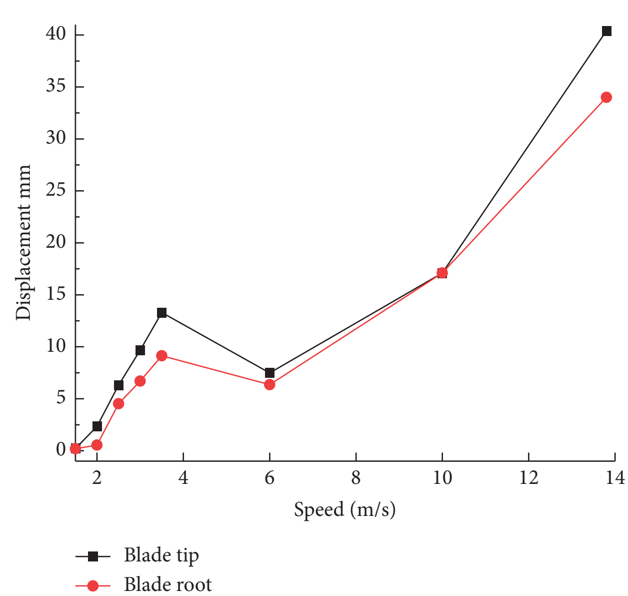

Figure 6: Displacement value curve of the blade tip and blade root.

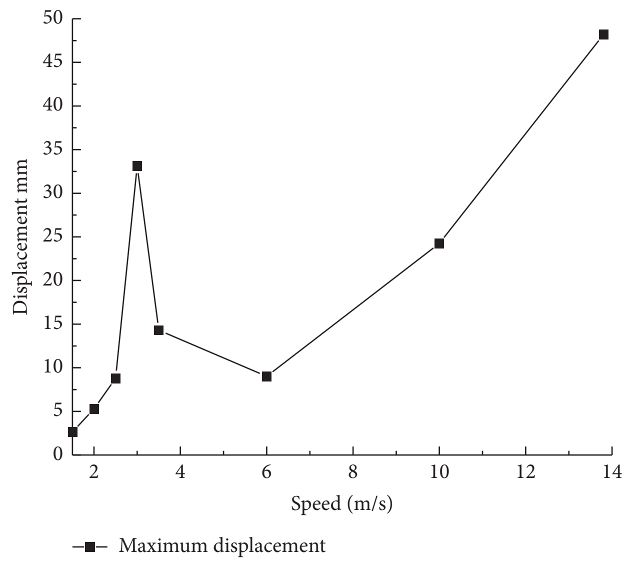

Figure 7: Maximum displacement curve.

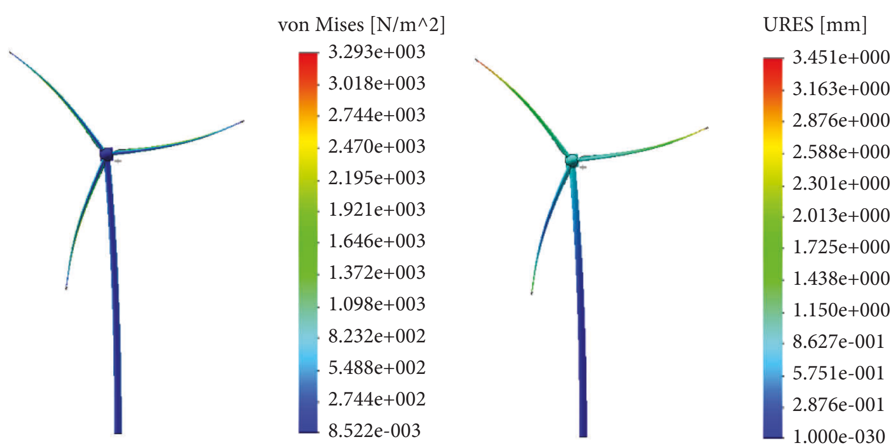

(a) (b)

Figure 8: . Dynamic response of 4428N. (a) Stress and (b) combined displacement.

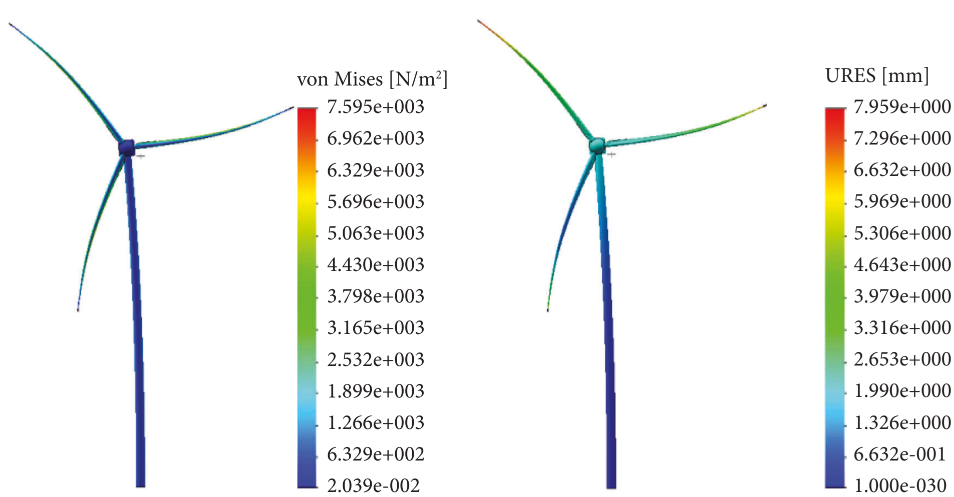

(a) (b)

Figure 9: . Dynamic response of 5784N. (a) Stress and (b) combined displacement.

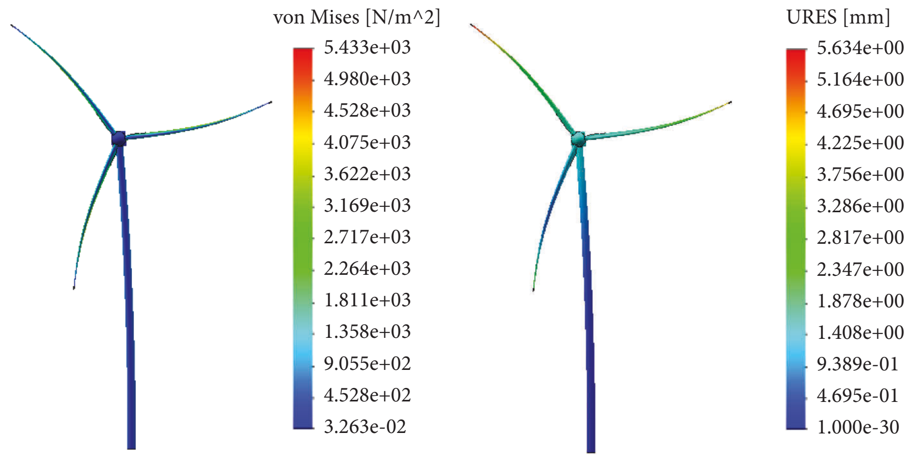

(a) (b)

Figure 10: . Dynamic response of 7320N. (a) Stress and (b) combined displacement.

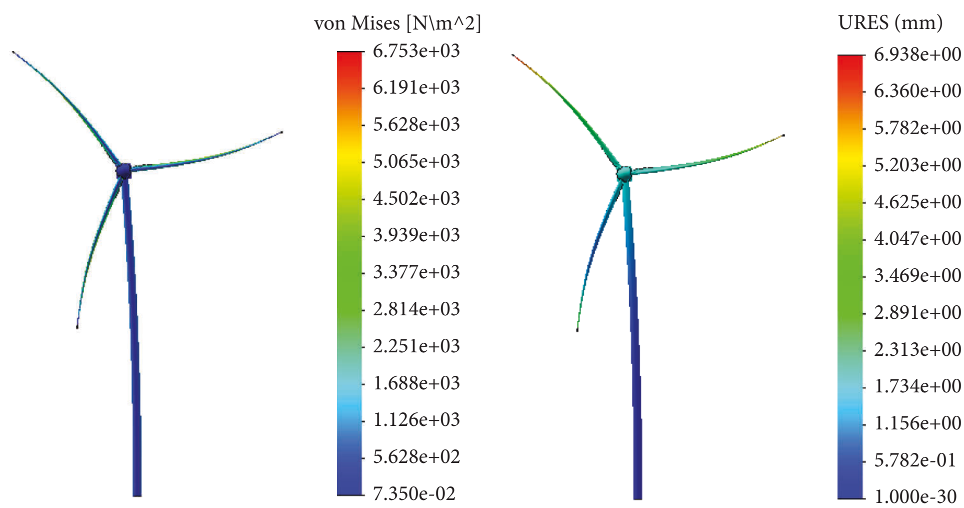

(a) (b)

Figure 11: . Dynamic response of 9037N. (a) Stress and (b) combined displacement.

In Figure 10, the maximum stress value of the wind turbine is 3533 Pa, which is located at the tip of the blade. The stress value at the middle and trailing edge of the blade is relatively small, and the stress range is 1811 Pa–3622 Pa. The stress value at other positions of the wind turbine is small, and the maximum displacement value is 5.634 mm, which is the same as the maximum stress position. The displacement decreases gradually with the decrease of the distance from the hub, and the displacement between the hub and the engine room area is 1.408 mm. In Figure 11, the maximum stress value of the wind turbine is 4102 Pa, which is located at the tip of the blade. The stress value at the middle and trailing edge of the blade is relatively small, and the stress range is 2251 Pa to 4502 Pa. The stress value at other positions of the wind turbine is small, and the maximum displacement value is 6.938 mm, which is the same as the maximum stress position. The displacement decreases gradually with the decrease of the distance from the hub, and the displacement between the hub and the engine room area is 1.734 mm.

5. Conclusions

To study the numerical response of a wind turbine under different wind speeds, a three-dimensional wind turbine structure model is established based on solid works, extracting the blade root and tip particles. Using finite element analysis, the results show that the tip, the blade root stress, and displacement under different wind speeds change with some regularity. It can provide a reference value for dynamic parameters of wind turbine operation and improve the stability of wind turbine operation.

(1) When the wind turbine is running, according to the trend of stress and displacement of blade tip and blade root, the change of blade structure is monitored so as to improve the stability of wind turbine operation.

(2) The changing trend of blade stress under different wind speeds shows a certain regularity. With the increase in wind speed, the blade stress and displacement are not monotonically increasing or decreasing functions but monotonically increasing in an interval at a certain wind speed, which is a critical point, or decreasing monotonically.

(3) Under different wind speeds, the stress and displacement of the tower, blade, and engine room change according to the detailed trend of the numerical analysis so as to provide a certain reference value for the stable operation of wind turbines [29].

Nomenclature

D: rotor diameter (m)

Abbreviations

URANS: Unreynolds-average Navier-stokes
CFD: Computational fluid dynamics
NREL: National renewable energy laboratory
WT: Wind turbine
HAWT: Horizontal-axis wind turbine
OWTs: Offshore wind turbines
GA: Genetic algorithms
MSDA: Multistandard decision analysis
ANP: Analysis of network processes
AMM: Alternating moment method
TSFP: Two-stage stochastic fuzzy programming.

Data Availability

The data that support the findings of this study are included within the article or its supplementary materials.

Conflicts of Interest

The authors declare that they have no conflicts of interest.

Acknowledgments

The research was supported by the Program for the Introduction of Foreign Intellects in Hebei Prov (2022) and "Research on Key Technologies and Equipment of Efficient and Clean Power Generation for Carbon Neutralization."

References

[1] W. H. Chen, J. B. Ocreto, J. S. Wang et al., "Two-stage optimization of three and four straight-bladed vertical axis wind turbines (sb-vawt) based on taguchi approach - sciencedirect," *e-Prime - Advances in Electrical Engineering, Electronics and Energy*, vol. 1, 2021.

[2] Hoang Quan Nguyen Ngoc, P. V. Lam, and Long Le Van, "Wind turbine blade design optimization using openfoam and dakota software[J]," *Transportation Research Procedia*, vol. 56, 2021.

[3] W. S. xin, Z. Liang dong, L. Cui, Z. H. ling, and J. D. sheng, "Numerical study of seabed response and liquefaction around a jacket support offshore wind turbine foundation under combined wave and current loading[J]," *Water Science and Engineering*, vol. 15, 2021.

[4] F. M. Massao, K. Haigh Stuart, and S. P. Madabhushi Gopal, "Comparison of the dynamic responses of monopiles and gravity base foundations for offshore wind turbines in sand using centrifuge modelling[j]. soils and foundations," *Soils and Foundations*, vol. 61, 2020.

[5] W. Shi, J. Han, C. Kim, D. Lee, H. Shin, and H. Park, "feasibility study of offshore wind turbine substructures for southwest offshore wind farm project in korea[J]," *Renewable Energy*, vol. 74, 2015.

[6] W. Carswell, J. Johansson, F. Løvholt et al., "Foundation damping and the dynamics of offshore wind turbine monopiles[J]," *Renewable Energy*, vol. 80, 2015.

[7] Z. R. Shu, Q. S. Li, and P. W. Chan, "Investigation of Offshore Wind Energy Potential in Hong Kong Based on Weibull Distribution function[J]," *Applied Energy*, vol. 156, 2015.

[8] Javier Serrano González,Manuel Burgos Payán,Jesús Riquelme Santos,Ángel Gaspar González Rodríguez, "Maximizing the overall production of wind farms by setting the individual operating point of wind turbines[J]," *Renewable Energy*, vol. 80, 2015.

[9] M. Karimirad and C. Michailides, "V-shaped semisubmersible offshore wind turbine: An alternative concept for offshore wind technology[J]," *Renewable Energy*, vol. 83, 2015.

[10] D. Micallef and T. Sant, "Loading effects on floating offshore horizontal axis wind turbines in surge motion," *Renewable Energy*, vol. 83, pp. 737–748, 2015.

[11] M. Ansari, M. R. H. Nobari, and E. Amani, "Determination of pitch angles and wind speeds ranges to improve wind turbine performance when using blade tip plates[J]," *Renewable Energy*, vol. 140, 2019.

[12] H. Dong Kim and S. G. Lee, "Reliability analysis of offshore wind turbine support structures under extreme ocean environmental loads[J]," *Renewable Energy*, vol. 79, 2014.

[13] L. Castro-Santos and V. Diaz-Casas, "Sensitivity analysis of floating offshore wind farms[J]," *Energy Conversion and Management*, vol. 101, 2015.

[14] M. Shafiee, "A fuzzy analytic network process model to mitigate the risks associated with offshore wind farms," *Expert Systems with Applications*, vol. 42, no. 4, pp. 2143–2152, 2015.

[15] C. Jung, D. Schindler, and L. Grau, "Achieving germany's wind energy expansion target with an improved wind turbine siting approach[J]," *Energy Conversion and Management*, vol. 173, 2018.

[16] Seyit Ahmet Akdağ and Ö. Güler, "Alternative moment method for wind energy potential and turbine energy output estimation[J]," *Renewable Energy*, vol. 120, 2018.

[17] A. Pacheco, E. Gorbeña, C. Sequeira, and S. Jerez, "An evaluation of offshore wind power production by floatable systems: a case study from sw portugal[J]," *Energy*, vol. 131, 2017.

[18] M. M. Savino, R. Manzini, Vincenzo Della Selva, and R. Accorsi, "A new model for environmental and economic evaluation of renewable energy systems: the case of wind turbines[J]," *Applied Energy*, vol. 189, 2016.

[19] C. Wang, H. Zhang, W. Fan, and P. Ma, "A new chaotic time series hybrid prediction method of wind power based on eemd-se and full-parameters continued fraction[J]," *Energy*, vol. 138, 2017.

[20] Z. Wang, A. Ozbay, W. Tian, and H. Hu, "An experimental study on the aerodynamic performances and wake characteristics of an innovative dual-rotor wind turbine[J]," *Energy*, vol. 147, 2018.

[21] S. Ahmad, A. Hassanzadeh, J. Jamali, M. Ali, and W.-H. Chen, "Determination of rated wind speed for maximum annual energy production of variable speed wind turbines[J]," *Applied Energy*, vol. 205, 2017.

[22] J. Zhao, Z.-H. Guo, Z.-Y. Su, Z.-Y. Zhao, X. Xiao, and F. Liu, "An improved multi-step forecasting model based on wrf ensembles and creative fuzzy systems for wind speed[J]," *Applied Energy*, vol. 162, 2016.

[23] Y. Chen, Li He, Li Jing, Xi Cheng, and H. Lu, "An inexact bi-level simulationoptimization model for conjunctive regional renewable energy planning and air pollution control for electric power generation systems[J]," *Applied Energy*, vol. 183, 2016.

[24] N. Zhang, A. Zhaoguang Hu, B. Shen, G. He, and Z. Yanan, "An integrated source grid load planning model at the macro level," *C_2017_Ene*, vol. 126.

[25] Q. Zheng, Q. Guo, H. Sun, Z. Pan, Y. Liu, and X. Wen, "An interval gas flow analysis in natural gas and electricity coupled networks considering the uncertainty of wind power[J]," *Applied Energy*, vol. 201, 2016.

[26] H. Dehra, "An investigation on energy performance assessment of a photovoltaic solar wall under buoyancy-induced and fan-assisted ventilation system[J]," *Applied Energy*, vol. 191, 2017.

[27] J. L. Zhen, G. H. Huang, W. Li, Z. P. Liu, and C. B. Wu, "An inexact optimization model for regional electric system steady operation management considering integrated renewable resources[J]," *Energy*, vol. 135, 2017.

[28] G. Palmer, "An input-output based net-energy assessment of an electricity supply industry[J]," *Energy*, vol. 141, 2017.

[29] T. Yu and F. P. A. Wu, "Modeling turbine wakes and power losses within a wind farm using les: an application to the horns rev offshore wind farm[J]," *Renewable Energy*, vol. 75, 2015.